Strain hardening in liquid-particle suspensions

J. Hyväluoma, P. Raiskinmäki, A. Koponen, M. Kataja, and J. Timonen
Department of Physics, University of Jyväskylä, FI-40014 Jyväskylä, Finland
(Received 10 June 2005; published 9 December 2005; corrected 23 February 2006)

The behavior of a liquid-particle suspension induced to sheared motion was analyzed by numerical simulations. When the velocity (strain) of the suspension began to increase, its viscosity first stayed almost constant, but increased then rapidly to a clearly higher level. This increase in viscosity is shown to be related to formation of clusters of suspended particles. Clusters are shown to increase the viscosity by enhanced momentum transfer though clustered particles. This is the mechanism behind the strain-hardening phenomenon observed in small-strain experiments on liquid-particle suspensions.

DOI: 10.1103/PhysRevE.72.061402 PACS number(s): 83.80.Hj, 47.15.Pn

I. INTRODUCTION

Complex fluids in the form of liquids with solid particles suspended in them are important in many fields of industry as well as in biological processes and in nature. Such suspensions exhibit a wide variety of complex rheological properties that are still relatively poorly understood in spite of the intensive research they have attracted. There is still obvious need for improving our understanding of many fundamental and complex phenomena that appear in liquid-particle suspensions.

Presence of solid particles in the fluid modifies the velocity field around these particles leading to an increase in the viscosity of the suspension. For dilute suspensions interactions between particles can be neglected, which leads to the famous Einstein formula [1] for the viscosity of the suspension. This formula predicts that the relative viscosity increases in the creeping-flow regime linearly with increasing solid-volume fraction, $\mu_r = 1 + 2.5\phi$ [1]. However, experiments show deviations from this simple result even at low solid-volume fractions ($\gtrsim 5\%$). Already at these concentrations close encounters of particles appear so frequently that many-body hydrodynamic interactions take effect.

There is increasing evidence that many phenomena exhibited by liquid-particle suspensions, which cannot be explained by effects produced by noninteracting suspended particles, are related to their microstructure, i.e., to spatial correlations of these particles. One form of spatial correlation is formation of clusters of suspended particles, which we already know [2] to have significant influence on the rheological properties of the suspension, although direct experimental demonstration of this influence has proved to be rather difficult [4–6]. As clusters we mean here compact groups of particles, formed as a result of hydrodynamic forces that bring suspended particles to close contact with each other. Short-range lubrication forces between these particles are then responsible for binding together such otherwise temporary aggregates.

Shear thickening, e.g., is a good example of a complex non-Newtonian phenomenon: For increasing particle shear-Reynolds number (defined below) dense suspensions exhibit increasing viscosity. For solid-volume fractions close to the maximum packing limit shear thickening may appear as an abrupt rise in viscosity, but for lower solid-volume fractions a continuously increasing viscosity is the most common behavior [3,4]. The prevalent conjecture for this shear-thickening behavior is formation of clusters of suspended particles (see, e.g., Refs. [4–7]). We have shown recently that, for low shear-Reynolds numbers, shear thickening is indeed related to enhanced momentum transfer through the particle phase of the suspension [2,8], while for Reynolds numbers above unity, inertial effects become significant [2].

A particularly interesting phenomenon observed in liquid-particle suspensions, which is related to shear thickening and has recently received experimental attention, is the so-called strain-hardening effect [9,10]: A significant and abrupt rise in viscosity is observed when an initially immobile suspension is induced to sheared motion. The prevailing belief is that also this phenomenon results from formation of particle clusters although no direct evidence of such clustering has so far been found. The strain-hardening phenomenon is present even in the simplest possible liquid-particle suspension, namely in that consisting of a Newtonian carrier fluid and non-Brownian and noncolloidal spherical particles. This kind of simple suspension was very recently analyzed in the detailed experiments by Carreau and Cotton [10]. Carreau and Cotton considered suspensions under steady shear. However, similar strain hardening has also be seen under oscillatory shear where an increase in viscosity is observer if the strain amplitude becomes large enough [11].

It is evident that in strain hardening some of the mechanisms responsible for increased viscosity in concentrated suspensions are expected to come into operation. Therefore, a more detailed understanding of the underlying mechanism behind strain hardening may also shed new light into structural issues that are more generally related to formation of viscosity in liquid-particle suspensions.

Computer simulations have widely been used for analyzing suspension flows. To this end several methods have been developed, and previously the technique mostly used was the method of Stokesian dynamics [12]. Other succesfully applied methods have been described in, e.g., Refs. [13–18], including the lattice-Boltzmann method [15] that has recently gained popularity and is also used in this work.

In this article we report results of our numerical simulations of the strain-hardening phenomenon in the simple suspension described above. We use the lattice-Boltzmann

method that has turned out to be an efficient tool for simulating complex fluids such as liquid-particle suspensions [15,19]. By numerical simulations we can gain detailed information about the microstructure of the suspension, and thereby seek a structural explanation for the experimentally observed strain-hardening phenomenon.

II. A LATTICE-BOLTZMANN METHOD FOR SUSPENSION SIMULATIONS

Flow of the carrier liquid in a suspension is governed by the Navier-Stokes equation. A recently introduced method for numerically simulating this equation is the lattice-Boltzmann (LB) method [19–21]. In the LB method a discrete version of the Boltzmann equation is solved on a regular grid for a single-particle distribution function $f_i(\mathbf{r},t)$ that describes the density of particles on lattice node $\mathbf{r}$ at time t with a discrete velocity $\mathbf{c}_i$. Of the several existing LB models [22–27] we use here the one based on the Bhatnagar-Gross-Krook (BGK) single-relaxation-time collision operator. In this model the dynamics of the system is governed by the LB equation

$$f_i(\mathbf{r}+\mathbf{c}_i,t+1) = f_i(\mathbf{r},t) + \frac{1}{\tau}[f_i^{eq}(\mathbf{r},t) - f_i(\mathbf{r},t)], \qquad (1)$$

in which f_i^{eq} is the equilibrium distribution function towards which the distribution functions are relaxed. This relaxation process is characterized by relaxation-time parameter τ. Notice that this equation as well as all the other equations and simulation results in this article are given in dimensionless lattice units. In the D3Q19 model [24] that we use here, the equilibrium distribution function can be expressed in the form

$$f_i^{eq} = \rho t_i \left[1 + \frac{\mathbf{c}_i \cdot \mathbf{u}}{c_s^2} + \frac{(\mathbf{c}_i \cdot \mathbf{u})^2}{2c_s^4} - \frac{u^2}{2c_s^2} \right], \qquad (2)$$

where t_i is a weight factor depending on the length of vector $\mathbf{c}_i$, $c_s = 1/\sqrt{3}$ is the speed of sound, ρ the density of the fluid, and $\mathbf{u}$ its velocity. Density ρ and velocity $\mathbf{u}$ are obtained from the zeroth and first velocity moments of the distribution function, respectively. Pressure is obtained from the equation of state, $p = c_s^2 \rho$, and kinematic viscosity is $\nu = (2\tau - 1)/6$. One of the advantages of the LB method is that the stress tensor can easily be determined locally at each lattice node,

$$\sigma_{\alpha\beta} = -p\delta_{\alpha\beta} - \left(1 - \frac{1}{2\tau}\right) \sum_i [f_i(\mathbf{r},t) - f_i^{eq}(\mathbf{r},t)] c_{i\alpha} c_{i\beta}. \qquad (3)$$

This property of the method is used in the stress analysis below.

In the LB method the no-slip boundary condition at the fluid-solid boundaries is most often realized by using the heuristic bounce-back rule in which the distribution that collides with a wall is simply reflected back. This boundary condition was generalized to moving boundaries by Ladd [25]. In the modified bounce-back rule the distribution f_i of the reflected particles is given by

$$f_i = f_{-i} + \frac{2\rho t_i}{c_s^2} \mathbf{u}_w \cdot \mathbf{c}_i. \qquad (4)$$

Here $-i$ denotes the link opposite to i and $\mathbf{u}_w$ is the local velocity of the moving boundary. This boundary condition is easy to implement and makes the simulation of particle suspensions straightforward. In addition to describing the effect of suspended particles on the fluid, it can also be used to compute the forces and torques acting on the particles, which are needed when updating the velocities, angular velocities, and positions of the particles. In the Ladd model particles were described as solid shells with an interior fluid [25]. An alternative approach was proposed by Aidun and Lu [28], in which there was no interior fluid. In our simulations a model without an interior fluid is used.

Long-range hydrodynamic interactions are correctly described by the LB method [15,29]. However, when particles are in close contact, this method fails to produce the form of the hydrodynamic interactions valid at very short distances between them [30]. It is, therefore, necessary to add a lubrication force between the particles of the form

$$\mathbf{F}_{\text{lub}} = -6\pi\mu \frac{a_1^2 a_2^2}{(a_1+a_2)^2} \left(\frac{1}{h} - \frac{1}{h_N} \right) \mathbf{U}_{12} \cdot \hat{\mathbf{R}}_{12} \hat{\mathbf{R}}_{12}, \qquad (5)$$

where μ is the dynamic viscosity of the fluid, a_1 and a_2 are the radii of the colliding particles, h is the shortest distance between them, h_N is a cut-off distance below which this force is used, $\mathbf{U}_{12} = \mathbf{U}_1 - \mathbf{U}_2$ is the velocity difference between the particles, and $\hat{\mathbf{R}}_{12}$ is a unit vector pointing from the center of particle 1 to that of particle 2. At short interparticle distances an additional lubrication force of this kind may, however, lead to large accelerations and thus to numerical instabilities.

An implicit updating scheme should thus be used for the particle velocities. On the other hand, this leads to numerical difficulties since such updating schemes have a complexity of $\mathcal{O}(n^3)$. Our approach to this problem is to set an upper limit to the lubrication force, and to use elastic collisions at very short interparticle distances. However, with this kind of particle handling overlaps may occasionally occur. Therefore, at small interparticle distances also a velocity-independent repulsive spring force [31,32] is added to avoid overlaps of particles [33]. Notice that this force is only used for particles that are expected to overlap, i.e., when the distance between the particles is below the threshold distance used for elastic collisions, and it is thus only rarely needed. Benchmark results for the simulation method applied in this work have been reported in Ref. [33], and they indicate the method to accurately produce the known viscosity behavior for liquid-particle suspensions.

To demonstrate the effect of the lubrication correction we show results of a simulation where two particles are approaching head on each others in a quiescent fluid. It is evident from Fig. 1 that, without a lubrication correction, the discreteness of the system prevents the computational method from detecting small changes at short distances in the interparticle separation, and thus from producing a divergent hydrodynamic force on the two particles.

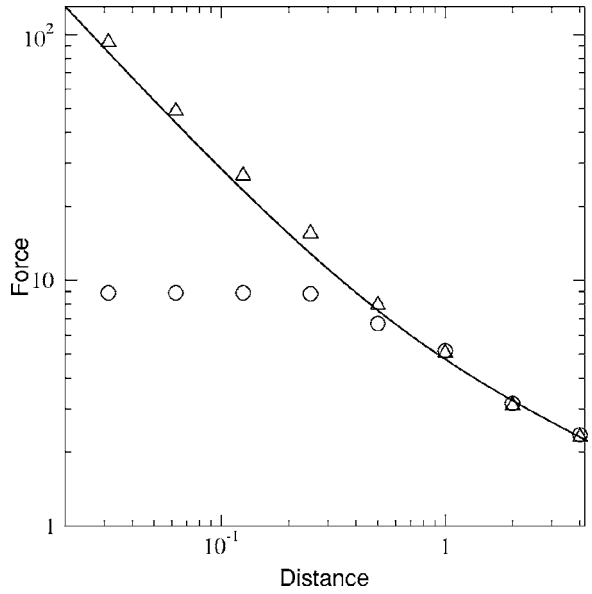

FIG. 1. Force on a particle approaching head on a similar particle as a function of the shortest distance between particle surfaces with (△) and without (○) a lubrication correction. Also shown is the force obtained from lubrication theory (solid line) [34]. Both quantities are expressed in lattice units.

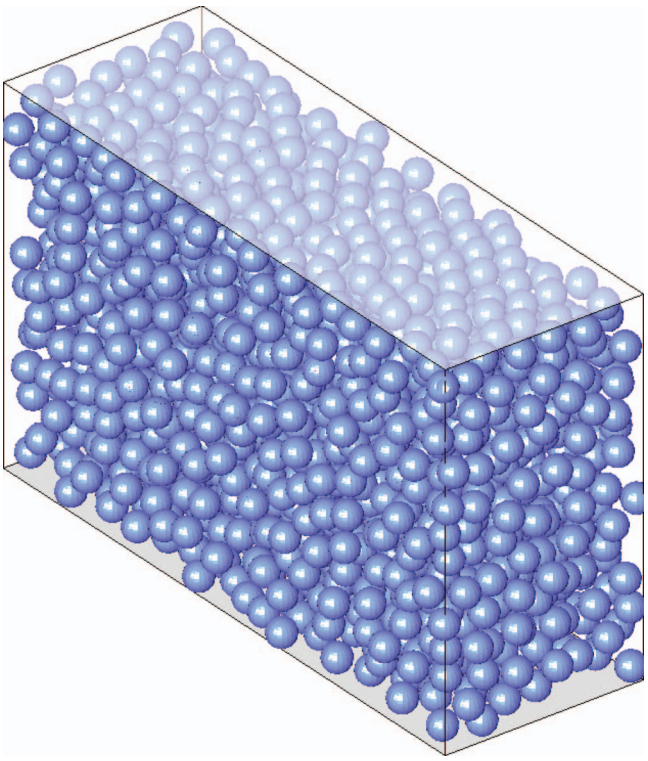

FIG. 2. (Color) Initial configuration of particles for a suspension with the solid volume fraction 0.41.

III. SIMULATION RESULTS FOR STRAIN HARDENING

Simulations were done in a plane Couette geometry in which the suspension is confined between two parallel plates. A shear flow was introduced by moving the plates in opposite directions with equal speed. The size of the system was $L_x \times L_y \times L_z = 90 \times 260 \times 158$ (in lattice units), where y is the flow direction and z the direction in which the velocity gradient was introduced; x is often called the vorticity direction. The simulated suspension consisted of spherical monodispersed particles with a diameter of $d=12$ lattice units. The solid volume fraction of the suspension varied between 0.41 and 0.56, and the number of particles between 1655 and 2270, respectively.

Carreau and Cotton [10] used a procedure they called "conditioning" in order to break the possible particle aggregates existing initially. In conditioning a low-strain-amplitude oscillatory flow was imposed in the sample before the actual strain-hardening measurements [10]. In simulations similar initial conditions were ensured by choosing such initial particle configurations in which no clusters were present (for our definition of a cluster, see below). Otherwise the initial particle configurations were random (see Fig. 2).

We simulated so-called start-up tests in which the shear rate was kept constant throughout the simulation. The plates were moved with such a speed that the resulting particle shear-Reynolds number,

$$\mathrm{Re}_p = \frac{d^2 2u_w}{L_z \nu}, \tag{6}$$

was $\mathrm{Re}_p \sim 1.6 \cdot 10^{-2}$. The measurements of Ref. [10] were done at extremely low shear-Reynolds numbers so that they varied in the interval $\mathrm{Re}_p \sim 10^{-11} - 10^{-9}$ [10]. The restrictions set simply by the CPU time available made simulations for such low values of Re_p impossible. Also, the system size in our simulations was smaller than that of Ref. [10] in which the distance between the plates was 100 particle diameters, whereas in our case it was about 13 particle diameters. Thus, we cannot expect an exact reproduction of the experimental results in our simulations, but this does not prevent us from semiquantitative comparison of the results, and from analyzing in particular the microscopic mechanism behind the strain-hardening phenomenon.

When a simulation is started, high velocity gradients arise close to the confining plates until a steady flow develops between them. These gradients cause high shear stresses on the plates, which would at least partially hide the strain-hardening phenomenon due to the relatively high shear-Reynolds number used in the simulations. In order to prevent this problem and to more closely comply with the experimental conditions, we initialized the simulations by holding the particles in their initial positions until a steady flow was developed (see Fig. 3). The velocities and angular velocities of the particles were, however, updated in the normal fashion during this initialization phase. When a steady state was reached, all particles were let to move at their current velocities and angular velocities, and the actual simulation of the system was thereby started.

In Fig. 4 we show the viscosities obtained from four start-up tests in which the solid-volume fractions were 0.41, 0.46, 0.51, and 0.56. Viscosity was determined from the shear forces acting on the plates by assuming a linear velocity profile between the plates in analogy with the experimental procedure. The results of these start-up tests displayed

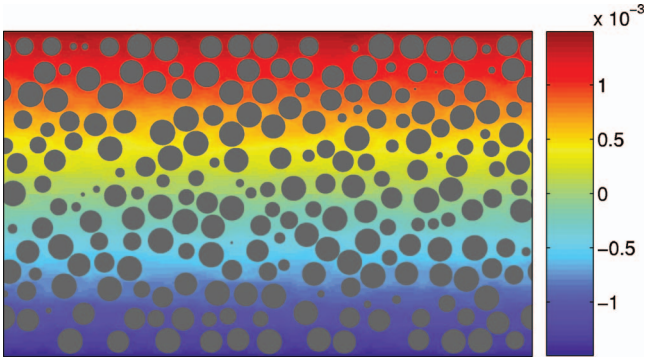

FIG. 3. (Color) A cross section of the velocity field after the initialization procedure for the suspension with the solid volume fraction 0.41.

strain-hardening behavior qualitatively similar to that observed in Ref. [10], i.e., a significant rise in viscosity was observed when the strain (i.e., maximal horizontal displacement of the fluid per unit height) reached a value of about 0.1. For decreasing solid-volume fraction the rise in the viscosity was also decreased, and it appeared at a somewhat lower strain. Fluctuations in the upper viscosity plateau were comparatively large due to the fairly small size of the simulated system.

We now demonstrate that the strain-hardening phenomenon results from changes in the microstructure of the suspension, which mainly appear as formation of particle clusters. We define a cluster such that particle i is considered to be in a cluster if in the same cluster there is a particle j such that

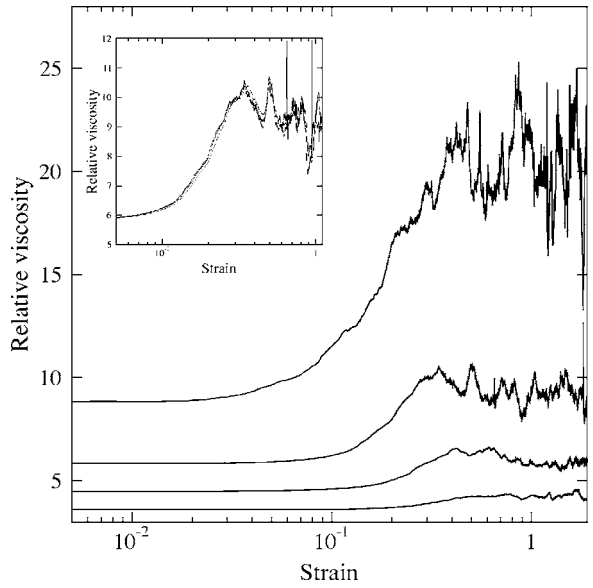

FIG. 4. Relative viscosity as a function of strain: Simulation results for solid-volume fractions 0.41, 0.46, 0.51, 0.56. The lowest (highest) curve is related to the lowest (highest) volume fraction of the suspension. In the inset shown is the relative viscosity of a suspension with the solid volume fraction ϕ=0.51 for three different shear rates.

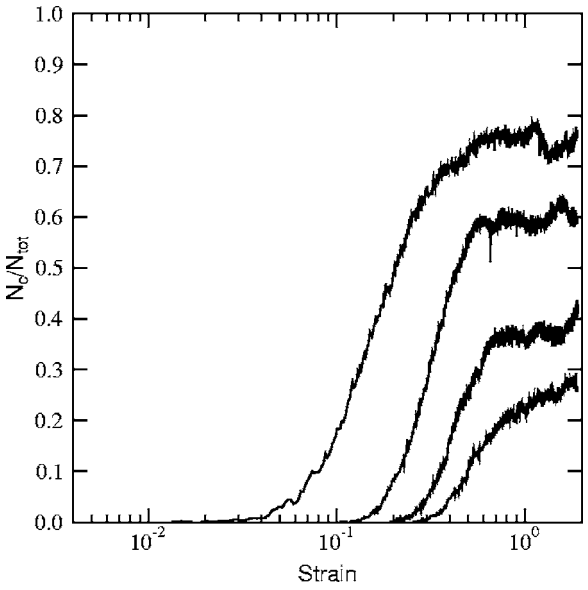

FIG. 5. Number of clustered particles as a function of strain. This result is for the same simulations as those shown in Fig. 4. N_c is the number of clustered particles and N_{tot} total number of particles.

$$|\mathbf{r}_i - \mathbf{r}_j| - a_i - a_j < \delta_c. \tag{7}$$

Here δ_c is a predefined treshold value for largest allowed distance between the nearest-neighbor particles in a cluster. In the analysis we performed the threshold value was δ_c=0.1 (lattice units). A rather strict definition for a cluster is needed due to the high solid volume fractions used in the simulations. However, a small variation in the threshold value would not change the qualitative behavior. We define the clustering rate as the proportion of the particles that belong to any of the clusters. This quantity does not describe all aspects of clustering and its effect on the apparent viscosity of the suspension: Also the size, shape, and orientation of the clusters may affect the viscosity. Clustering rate will, however, give a qualitative picture of the clustering process. In Fig. 5 we show the number of clustered particles as a function of strain for the same simulations for which the viscosities were shown in Fig. 4. It is evident that clustering rate behaves similarly to viscosity. When the solid-volume fraction of the suspension is increased, clustering and the rise in viscosity both appear at a smaller value of strain. It is evident that for increasing concentration the mean interparticle distance becomes smaller, which enhances clustering.

Experiments indicate that the viscosity of the suspension is independent of the shear rate in the regime of very low rates [9,10]. We, therefore, considered the behavior of our model suspension with a solid-volume fraction of ϕ=0.51 for three different shear rates. Notice that in all these simulations exactly the same initial configuration of particles was used. We found that the behavior of viscosity was almost identical for the three shear rates (cf. the inset in Fig. 4). This indicates that strain hardening is indeed connected to the microstructure of the suspension.

Consider now momentum transfer in the above suspensions. The lattice-Boltzmann method is ideal for this kind of

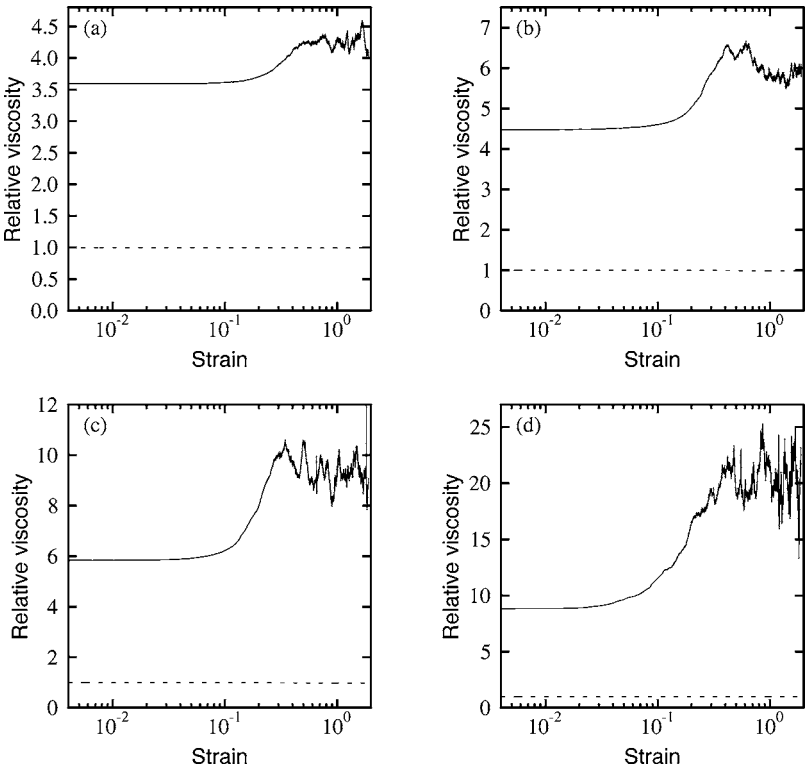

FIG. 6. Relative viscosity as a function of strain: (a) ϕ=0.41, (b) ϕ=0.46, (c) ϕ=0.51, and (d) ϕ=0.56. Dotted lines indicate the proportion of viscosity that results from fluid stress.

analysis since the deviatoric stress tensor can be calculated locally from the nonequilibrium part of the distribution function, and no approximation is needed for derivatives of the local velocity. The stresses that originate from the fluid and the solid phase can be determined separately, and we did so in each plane parallel to the moving plates. We thus determined the proportion of viscosity that results from momentum transfer through the fluid phase, averaged over all planes. The rest of the viscosity results from the internal stresses of the particles since the convective stresses were found to be insignificant in both the fluid and the solid phase. Results of this stress analysis is shown in Fig. 6. It is evident from this figure that the observed increase in viscosity, i.e., the strain-hardening effect, is caused by enhanced momentum transfer via the solid phase.

We still need to verify that the enhanced momentum transfer via the solid phase is indeed dominated by clusters of particles. To this end we determined the internal stress for each individual particle. This was done by integrating the forces acting on the surfaces of the particles. The resulting components of the stress tensor averaged over a particle are given by

$$\langle \sigma_{\alpha\beta} \rangle = \frac{1}{2V} \oint_S (P_\alpha x_\beta + P_\beta x_\alpha) \mathrm{d}S, \tag{8}$$

where V is the volume of the particle, $\mathbf{P}$ the external force per unit area acting on particle surface, and $\mathbf{x}$ the position vector [35]. This force is directly obtained from the fluid-solid boundary condition imposed [Eq. (4)]. Since we know from the cluster analysis which particles belong to clusters, we can determine the average internal shear stresses in clustered and nonclustered particles using the stresses of individual particles obtained by using Eq. (8). Figure 7 shows that the stresses in the clustered particles are considerably higher than those in the nonclustered particles. We can thus conclude that formation of particle clusters is indeed responsible for the strain-hardening phenomenon.

IV. DISCUSSION AND CONCLUSIONS

In this work we simulated the behavior of a liquid-particle suspension with noncolloidal and non-Brownian solid par-

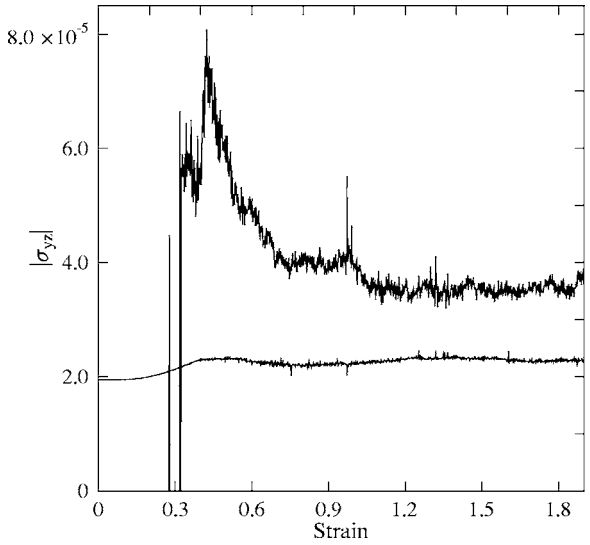

FIG. 7. Mean internal stress of clustered (upper curve) and nonclustered particles (lower curve) for ϕ=0.41. There were no clustered particles initially.

ticles using the LB method. The strength of computer simulations in studying correlated structures inside suspensions, which may significantly affect their rheological behavior, is that simulations make it possible to analyze in detail the microscopic structure of the suspension. They thus provide direct information that would be difficult to obtain by experimental techniques. In addition to the structural information, the LB method enables computation of the internal stresses of individual particles as well as the local components of the stress tensor in the fluid. These features of the method enable, e.g., an exact analysis of various momentum transfer mechanisms that are responsible for changes in the viscosity of the suspension.

With these methods we analyzed the viscosity of a liquid-particle suspension that is immobile initially but is then induced to sheared motion. At the early phases of the process, the viscosity of the suspension stayed almost constant, but increased then fairly rapidly to a clearly higher level. We showed that this rise in viscosity is accompanied by formation of clusters of suspended particles. A detailed analysis of momentum transfer in the system revealed that increasing viscosity is caused by increasing momentum transfer via suspended particles. Finally we demonstrated that momentum transfer is dominated by particles that belong to clusters. We could thereby explain the mechanism that creates the so-called strain-hardening phenomenon observed [10] in detailed small-strain experiments on liquid-particle suspensions.

It is evident that the clustering tendency of suspended particles, shown here to be responsible for the strain-hardening phenomenon, is also more generally a mechanism that causes the viscosity of the suspension to increase for increasing shear-Reynolds number, before inertial effects begin to play a dominant role [2]. The first results for two-dimensional suspensions, which indicated such a role for particle clusters [2,8], are thus carried over to three dimensions. The momentum transfer analysis carried out here is also more detailed than the one reported in Ref. 8.

[1] A. Einstein, Ann. Phys. **19**, 289 (1906); **34**, 591 (1911).
[2] P. Raiskinmäki, J. A. Åström, M. Kataja, M. Latva-Kokko, A. Koponen, A. Jäsberg, A. Shakib-Manesh, and J. Timonen, Phys. Rev. E **68**, 061403 (2003).
[3] H. M. Laun, R. Bung, S. Hess, W. Loose, O. Hess, K. Hahn, E. Hädicke, R. Hingmann, F. Schmidt, and P. Lindner, J. Rheol. **36**, 743 (1992).
[4] P. d'Haene, J. Mewis, and G. G. Fuller, J. Colloid Interface Sci. **156**, 350 (1993).
[5] J. W. Bender and N. J. Wagner, J. Rheol. **40**, 899 (1996).
[6] B. J. Maranzano and N. J. Wagner, J. Chem. Phys. **114**, 10514 (2001).
[7] J. R. Melrose and R. C. Ball, J. Rheol. **48**, 937 (2004); **48**, 961 (2004).
[8] A. Shakib-Manesh, P. Raiskinmäki, A. Koponen, M. Kataja, and J. Timonen, J. Stat. Phys. **107**, 67 (2002).
[9] F. Gadala-Maria and A. Acrivos, J. Rheol. **24**, 799 (1980).
[10] P. J. Carreau and F. Cotton, in *Transport processes in bubbles, drops, and particles*, 2nd ed., edited by D. De Kee and R. P. Chhabra (Taylor & Francis, New York, 2002), pp. 397–425.
[11] S. R. Raghavan and S. A. Khan, J. Colloid Interface Sci. **185**, 57 (1997).
[12] J. F. Brady and G. Bossis, Annu. Rev. Fluid Mech. **20**, 111 (1988).
[13] H. Tanaka and T. Araki, Phys. Rev. Lett. **85**, 1338 (2000).
[14] K. Höfler and S. Schwarzer, Phys. Rev. E **61**, 7146 (2000).
[15] A. J. C. Ladd and R. Verberg, J. Stat. Phys. **104**, 1191 (2001).
[16] H. H. Hu, N. A. Patankar, and M. Y. Zhu, J. Comput. Phys. **169**, 427 (2001).
[17] R. Glowinski, T. W. Pan, T. I. Hesla, D. D. Joseph, and J. Périaux, J. Comput. Phys. **169**, 363 (2001).
[18] Y. Nakayama and R. Yamamoto, Phys. Rev. E **71**, 036707 (2005).
[19] S. Chen and G. D. Doolen, Annu. Rev. Fluid Mech. **30**, 329 (1998).
[20] D. H. Rothman and S. Zaleski, *Lattice-Gas Cellular Automata* (Cambridge University Press, Cambridge, 1997).
[21] S. Succi, *The Lattice Boltzmann Equation for Fluid Dynamics and Beyond* (Oxford University Press, Oxford, 2001).
[22] G. R. McNamara and G. Zanetti, Phys. Rev. Lett. **61**, 2332 (1988).
[23] F. J. Higuera and J. Jimènez, Europhys. Lett. **9**, 663 (1989).
[24] Y. H. Qian, D. d'Humieres, and P. Lallemand, Europhys. Lett. **17**, 479 (1992).
[25] A. J. C. Ladd, J. Fluid Mech. **271**, 285 (1994); **271**, 311 (1994).
[26] P. Lallemand and L. S. Luo, Phys. Rev. E **61**, 6546 (2000).
[27] D. d'Humieres, I. Ginzburg, M. Krafczyk, P. Lallemand, and L. S. Luo, Philos. Trans. R. Soc. London, Ser. A **360**, 437 (2002).
[28] C. K. Aidun and Y. Lu, J. Stat. Phys. **81**, 49 (1995).
[29] A. Jäsberg, A. Koponen, M. Kataja, and J. Timonen, Comput. Phys. Commun. **129**, 196 (2000).
[30] N. Q. Nguyen and A. J. C. Ladd, Phys. Rev. E **66**, 046708 (2002).
[31] R. C. Ball and J. R. Melrose, Adv. Colloid Interface Sci. **59**, 19 (1995).
[32] J. Kromkamp, D. T. M. van den Ende, D. Kandhai, R. G. M. van der Sman, and R. M. Boom, J. Fluid Mech. **529**, 253 (2005).
[33] J. Hyväluoma, P. Raiskinmäki, A. Koponen, M. Kataja, and J. Timonen, J. Stat. Phys. **121**, 149 (2005).
[34] D. J. Jeffrey and Y. Onishi, J. Fluid Mech. **139**, 261 (1984).
[35] L. D. Landau and E. M. Lifshitz, *Theory of Elasticity*, 2nd English ed. (Pergamon, Oxford, 1970).